AMPLITUDE OF RIPPLING IN THE P_β PHASE OF DIPALMITOYLPHOSPHATIDYLCHOLINE BILAYERS

J. STAMATOFF, B. FEUER, H. J. GUGGENHEIM, G. TELLEZ, AND T. YAMANE
Bell Laboratories, Murray Hill, New Jersey 07974

ABSTRACT We present x-ray diffraction results of dipalmitoylphosphatidylcholine (DPPC) multilayers in three structural phases. Using pure DPPC, precision temperature control, and high angular resolution methods, we have discovered splitting of the first diffraction order due to multilayering in the P_β phase. This splitting permits us to calculate the amplitude of ripples in this phase. The amplitude is large enough to suggest a structural mechanism for rippling.

INTRODUCTION

Intensive investigation of the structure of lipid mesophases has provided major insights into the structure of biological membranes. These mesophases are functions of the thermodynamic variables of temperature, pressure, and water content. For example, L-α-dipalmitoylphosphatidylcholine (DPPC) forms three multilayered structures with >5% water content and between 20° and 70°C.

Tardieu et al.[1] showed that x-ray diffraction of lipid dispersions provides a powerful tool to identify phases, determine phase transitions, and, in many cases, describe the general structure of each phase. It is remarkable that this wealth of information is available from unorientated samples.

Using Luzzati's notation, x-ray studies have shown that the phase diagram for DPPC consists of three phases: $L_{\beta'}$, P_β and L_α. The low temperature-low water content phase, $L_{\beta'}$, consists of multilayers of flat lipid bilayer sheets in which the hydrocarbon chains are tilted with respect to the bilayer normal. The high temperature phase, L_α, extends from low to high water content. It also is multilayered and consists of flat bilayers in which the hydrocarbon chains are disordered (or melted). Thus, the L_α phase is liquid crystalline. The transition between the $L_{\beta'}$ and L_α phases is known as the main transition.

Above 20% water content, a second lower enthalpy and broader transition occurs at ~34°C. This transition is known as the pretransition. Between the pretransition and main transition (at ~42°C for this water content range) occurs the third phase known as P_β. The transition between P_β and L_α has recently been studied at high water contents by precision calorimetric methods that suggest that the transition is first order (2). Optical methods have also been used to determine the entire phase diagram (3).

Janiak et al. (4) showed that the P_β phase consists of rippled multilayers. This observation was confirmed by electron microscopic studies (Luna and McConnel [5]). The rippled structure was observed earlier by Tardieu et al. (1) on short chain lecithins. Rand et al. (6) showed that the hydrocarbon chains became parallel to the stacking direction by investigating multilayer periodicity changes and the line shape of the $(4.2\ \text{Å})^{-1}$ reflection. Graddick et al. (7) showed increased disorder for stacking in both pure DPPC in excess water and multilayers in excess $CaCl_2$ solutions.

In this study, we find that, at higher angular resolution, the first diffraction order (1,0) due to multilayer formation, is resolved into two peaks. We find that the (h,0) diffraction orders due to multilayering, are significantly broadened as discovered earlier (7). We suggest that the two peaks about the (1,0) reflection, are due to a zero in the structure factor curve of the rippled bilayer. We show that this zero implies that the amplitude of rippling is ~25 Å (or that the total ripple displacement is ~50 Å or one bilayer width). This is consistent with an average displacement of ~2.5 Å (or one CH_2 group) for each hydrocarbon chain.

MATERIALS AND METHODS

DPPC was prepared according to the method of Albon and Sturtevant (2). Palmitic acid (PA) was zone refined to remove impurities from other fatty acids. Palmitic anhydride was prepared from the reaction of PA with *N,N'*-dicyclohexylcarbodiimide (Sigma Chemical Co., St. Louis, MO) (2:1 molar ratio) in anhydrous carbon tetrachloride for 5 h at room temperature (8). The yield was stoichiometric. Potassium palmitate was found by the reaction of PA solubilized in methanol with an equal molar quantity of methanolic potassium hydroxide. The salt was obtained by rotary evaporation of the solvent. L-α-glycerolphosphoryl choline (GPC) was obtained from egg yolk lecithin that was column chromatographed on aluminum oxide, Brockmann No. 4 (~10% water by weight) (Camag Inc., New Berlin, WI) (9). The lecithin was treated with methanolic *t*-butyl-ammonium hydroxide (Eastman Kodak Co., Rochester, NY) for

Dr. Stamatoff's present address is Celanese Research Co., Summit, NJ; Dr. Feuer's is Exxon Research and Engineering Co., Linden, NJ; Dr. Tellez's is Chemistry Department, University of Texas at El Paso, El Paso, TX.

2 h at room temperature to cleave off the fatty acid residues. GPC was precipitated from this reaction with ether and crystallized as the cadmium chloride salt (10). The cadmium chloride was removed by passing a 2% aqueous solution over a mixed-bed resin consisting of IR-45 and IRC-50 (Mallinckrodt Inc., St. Louis, MO). The resulting ion-free solution was rotary evaporated, and then lyophilized GPC crystals were obtained from an ethanol-ether solvent system. DPPC was synthesized by heating at 80°C *in vacuo* a mixture of palmitic anhydride, potassium palmitate, and GPC in molar ratios of 7:9:5 in a round flask for ~3 d (2,11). The progress of the reaction was monitored by thin layer chromatographic separations using silica gel on glass plates (F-254, EM Laboratories, Inc., Elmsford, NY; solvents, chloroform:methanol:water:glacial acetic acid, 65:25:4:1 by volume). The spots were visualized with molybdophosphoric acid spray (EM Laboratories). Purification of DPPC was achieved by multiple chloroform and ether extractions followed by column chromatography on aluminum oxide (9), and purity was checked using the thin layer chromatography system and by elemental analysis.

Dry DPPC was weighed and mixed with triple-distilled deionized water using a microliter syringe. Following Janiak et al.(4), the samples were heated above the main transition and centrifuged repeatedly through a small constriction. The samples were then sealed under N_2 in 1.0-mm quartz x-ray capillary tubes. For diffraction studies, a sample was placed in an evacuated oven with mylar windows. An inner shield about the sample served to reduce temperature gradients. Temperature was controlled to ± 0.010°C by a model DTC-500 sp controller (Lakeshore Cryotronics, Inc., Eden, NY). Gradients across the sample were measured using a platinum resistance thermometer. Gradients were found to be <0.200°C in this study.

X rays were obtained from a rotating anode generator operating at 4 kW with a 0.2 × 0.2 mm^2 projected source size. X rays were monochromatized and focused to a 1.0 × 0.2 mm^2 spot, using a bent quartz monochromator. The $10\bar{1}1$ quartz crystal was asymmetrically cut at 6° relative to these planes. The monochromator was tuned for $CuK_{\alpha 1}$ x rays (λ = 1.540 Å) for this study.

Diffracted x rays were recorded using a stable position sensitive x ray detector. The linear detector is filled with Ar—CH_4 at 100 lb/in^2 and is ~90% efficient. The detector uses a nichrome wire anode and charge division position encoding. The resolution of the detector is 0.5 mm (full width at half maximum) along its 10-cm length.

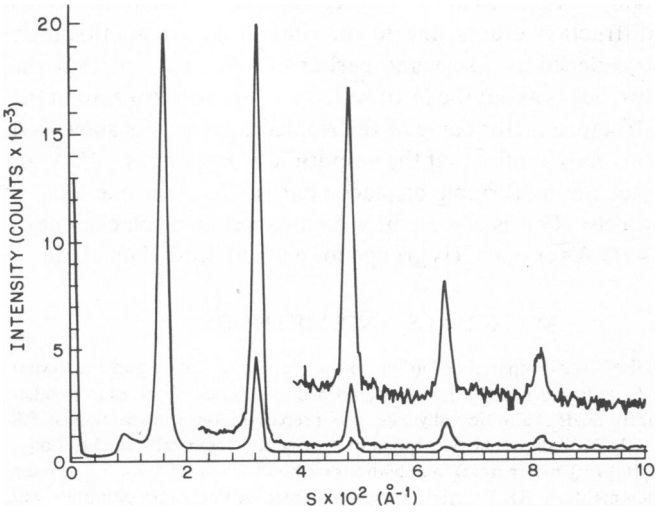

FIGURE 1 Small angle x-ray diffraction patterns of L-α-dipalmitoylphosphatidylcholine (DPPC) at lower angular resolution. The unoriented multilayer sample contains 35% water and is at 24.7°C. A different oven that provided poorer temperature control (± 0.5°C) was used. Reflections due to stacking of the lipid bilayers are apparent to ~(10 Å)$^{-1}$. These reflections do not indicate disorder and higher diffractions orders remain sharp. DPPC is in the $L_{\beta'}$ phase under these conditions.

The sample to detector distance was 141.1 cm. This is unusually long and provided significantly improved angular resolution. Our angular resolution is dominated by the position resolution of the detector. The resolution is $\Delta 2\theta$ = 0.5 mm/1411 mm radians (or 0.02°) for the scattering angle.

Wide angle diffraction scans were recorded using a 60 kW x-ray generator and a Picker (Picker Corp., Cleveland OH) diffractometer. The same oven was used to control temperature.

RESULTS

Before describing the high angular resolution x-ray diffraction results, lower angular resolution data that were collected at a more conventional sample-to-detector distance of 305 mm will be presented. The lower angular resolution data provides a view of a larger region of reciprocal space. Fig. 1 shows the diffraction pattern from a 35% water content sample at 24.7°C. DPPC is in the $L_{\beta'}$ phase at these conditions. Fig. 2 shows expansions of the

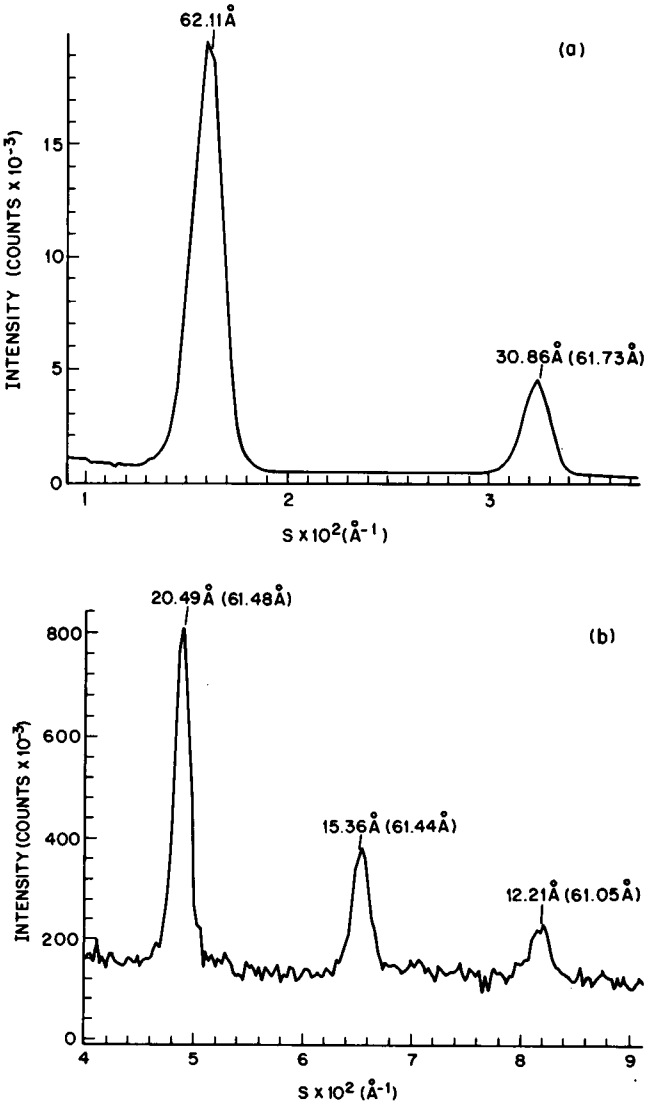

FIGURE 2 Indexing of the x-ray diffraction pattern shown in Fig. 1. Bragg spacings are indicated. Layer spacings computed from each Bragg spacing are also given. (*a*) h = 1,2; (*b*) h = 3–5.

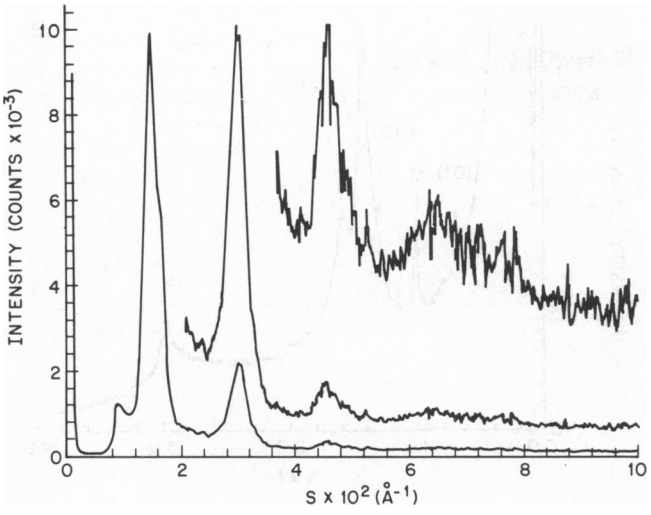

FIGURE 3 Small angle x-ray diffraction patterns of DPPC at lower angular resolution in the P_β phase. The unoriented multilayer sample contain 35% water and is at 37.5°C. A different oven that provided poorer temperature control was used. Reflections due to stacking of the lipid bilayers are apparent to ~(10 Å)$^{-1}$. These reflections do indicate disorder and are significantly broader than those shown in Fig. 1 for the $L_{\beta'}$ phase. At these higher water contents, numerous reflections due to rippling are not observed (see Figs. 5 and 6). Two peaks in the first diffraction order region are indicated.

same pattern and Bragg spacings of the orders are indicated. The calculated layer spacing is also given for each order showing the limited accuracy of these results.

Fig. 3 shows the diffraction pattern from the same 35% water content sample at 37.5°C. DPPC is in the P_β phase under these conditions. A considerable increase in disorder is noted as previously determined (7). Peaks due to rippling at this water content are not apparent as are found for dimyristoyl lecithin (DML) at 22.3% water content and at 20°C (12). Rather, two peaks appear in the first-order position. Indexing of this pattern is shown in Fig. 4. The peaks in the first-order region occur at Bragg spacings on either side of the layer spacing calculated from the second or third orders. In addition to the lack of numerous peaks due to rippling found at lower water content for DML (4,12) or DPPC (4), the Bragg spacings calculated from the P_β pattern shown in Fig. 3 and 4 suggest that the two peaks in the first-order region are not simply two reflections of a monoclinic lattice formed by a rippled multilayer.

Higher angular resolution results obtained using a sample-to-detector distance of 141.1 cm provide further insight. Fig. 5 shows three patterns in $L_{\beta'}$, P_β, and L_α for a 45% water content sample and a pattern in P_β for a 25% sample. Peaks due to stacking of the multilayers are indexed as $(h,0)$. In plane peaks due to rippling are indexed as (h, k) $(k \neq 0)$. The patterns in Fig. 5 extended to just beyond the (2,0) reflection. Several phenomena that have been previously observed are noted. First, peaks due to rippling are observed in P_β (4,12). Second, an increase in periodicity in P_β is found (4,6). Finally, increased disorder in P_β is noted (7). In addition, two peaks are observed in the (1,0) region.

Fig. 6 shows five water contents, (25, 35, 45, 60, and 75%) at 37.5°C and an expanded view of the first-order region. Two peaks that do not index on the (h, k) lattice replace the (1,0) reflection for all water contents. For this discussion, the phenomenon will be referred to as splitting of the (1,0) reflection. Thermal studies of these samples show that this splitting extends throughout the P_β region (from 35° to 42°C). The phenomenon occurs upon heating from the $L_{\beta'}$ phase or cooling from the L_α phase.

Fig. 7 shows wide angle diffraction scans of the (4.2 Å)$^{-1}$ region. In agreement with Rand et al. (6), we find that the line shape changes from an asymmetric peak ($L_{\beta'}$) to a symmetric peak (P_β), to a broad diffraction band (L_α).

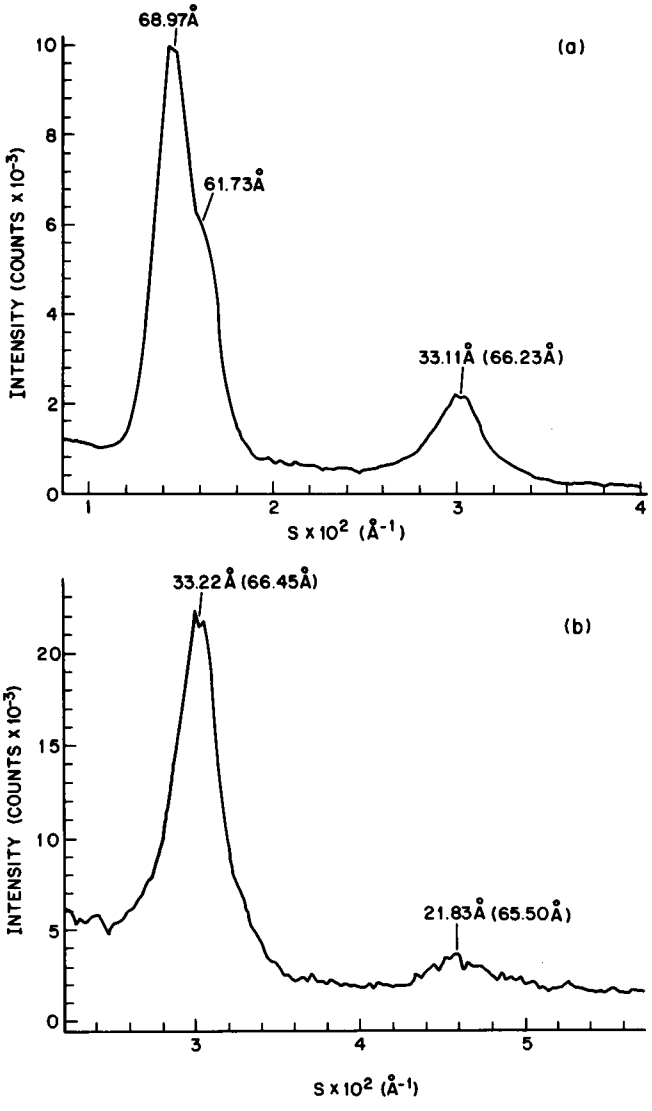

FIGURE 4 Indexing of the x-ray diffraction pattern shown in Fig. 3. Bragg spacings are indicated. Layer spacings computed from each Bragg spacing are also given. The two peaks in the first-order region are on either side of the predicted position given by higher diffraction orders. (*a*) $h = 1, 2$. (*b*) $h = 2, 3$.

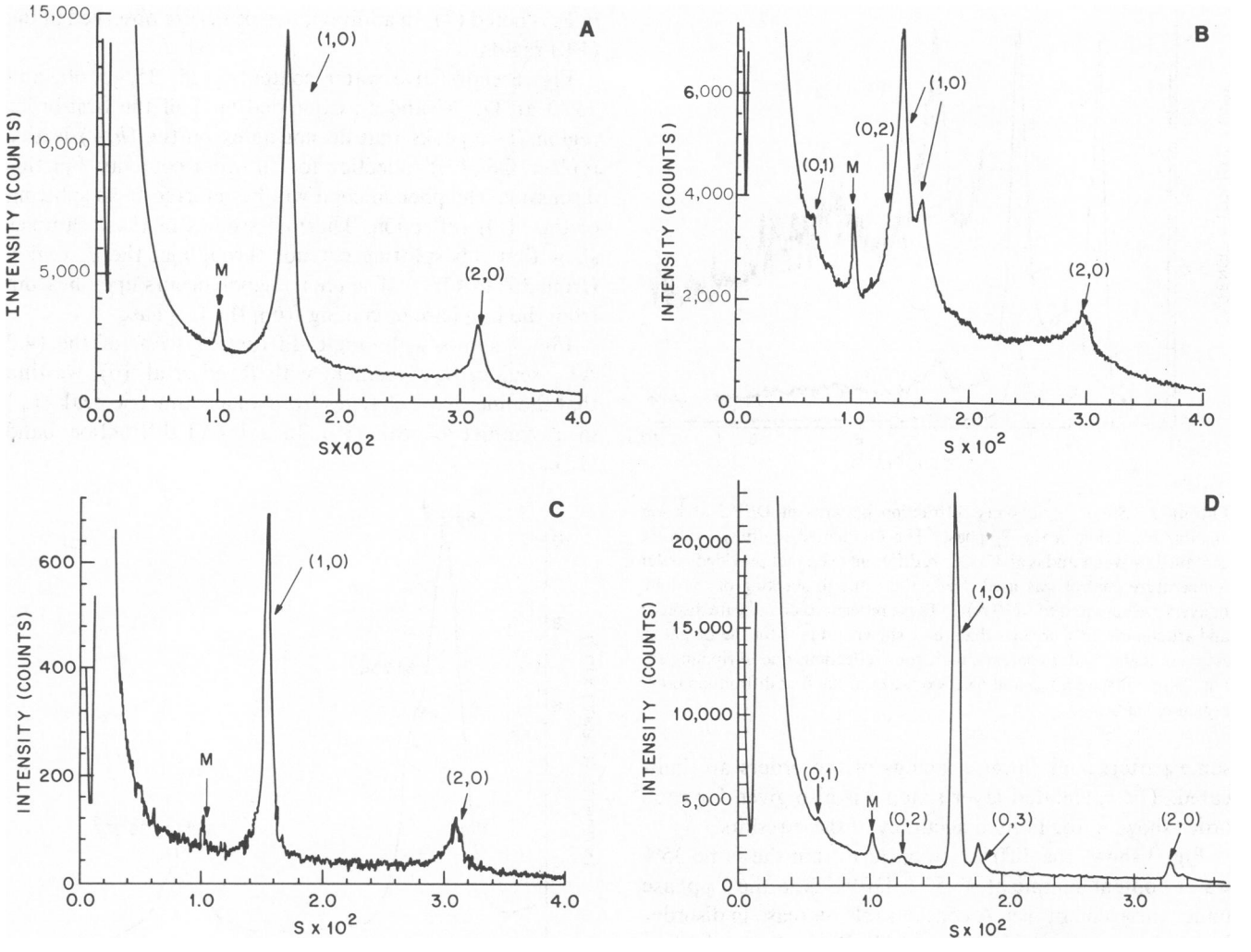

FIGURE 5 Small angle diffraction patterns of DPPC at higher angular resolution. (*a*) $L_{\beta'}$ phase at 27.3°C and 45% water content, (*b*) P_β phase at 37.5°C and 45% water content, (*c*) L_α phase at 46.0°C and 45% water content, and (*d*) P_β phase at 37.5°C and 25% water content. The abscissa is in units for $S = (2\sin\theta)/\lambda$ where 2θ is the scattering angle. Reflections are indexed as described in the text. A peak in the background due to a weak reflection from the bent quartz monochromator is marked *M*. This peak is not due to lipid diffraction.

DISCUSSION

Our results suggest, as first described by Rand et al. (6), that the tilted hydrocarbon chains of the $L_{\beta'}$ phase become parallel to the stacking axis in the P_β phase. In agreement with Janiak et al. (4,12), we find peaks that are due to rippling of the bilayer. Finally, in agreement with Graddick et al. (7), we find increased disorder of the multilayer as evidenced by the increased peak widths.

Splitting of the (1,0) reflection is a phenomenon that has not been previously observed. Even though the phenomenon is suggested by the lower angular resolution studies (Figs. 1–4), splitting is clearly demonstrated by the increased angular resolution of our experiment. The increased width of the lamellar reflections in the P_β region make observation of this splitting impossible at lower angular resolution for the 25% water content case.

The existance of two peaks in the (1,0) region is not due to the coexistance of two phases. First, the wide angle scans (Fig. 3) do not suggest two hydrocarbon chain states, as would be observed if, for example, L_α were coexisting with $L_{\beta'}$. Second, our thermodynamic system consists of $N(=2)$ components (DPPC and water), and L phases. Measurements of 45–75% show an additional water uptake of the lipid (as evidenced by increased periodicity or increased peak width) and, thus, demonstrate that an excess water phase exists. If there were two lipid-water phases coexisting, then, counting excess water and the vapor phase in the sealed capillary, the total number of phases would be four. Using Gibbs's phase rule, the number of thermodynamic degrees of freedom would be: $F = N + 2 - L = 2 + 2 - 4 = 0$. The fact that the split peaks exist over a range of temperatures proves that the new peak is not due to a new phase.

Tables I and II summarize data taken in the three states as a function of water content. As must be the case, the (1,0) reflection is half the distance from the origin of reciprocal space as the (2,0) reflection in the $L_{\beta'}$ and L_α

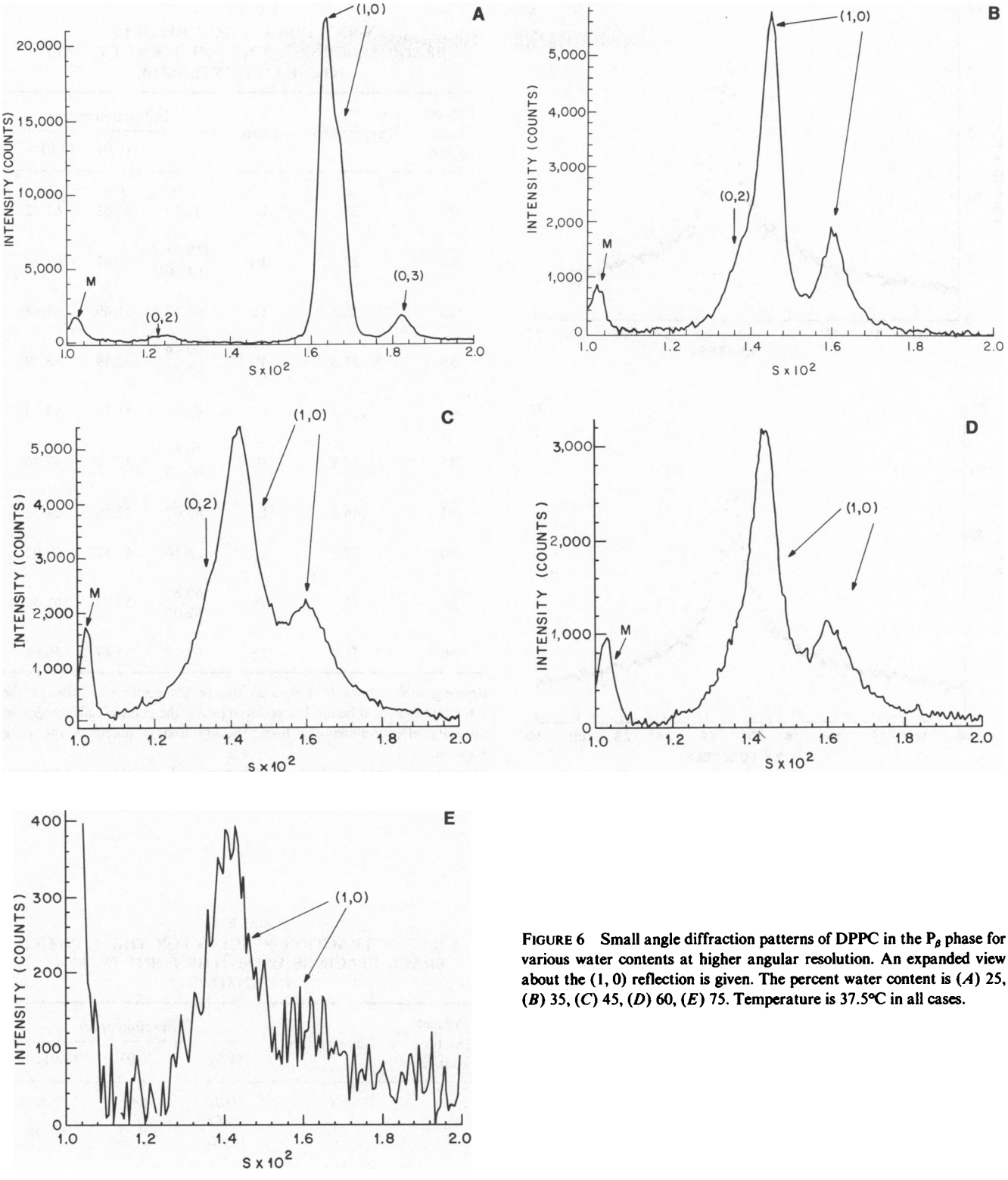

FIGURE 6 Small angle diffraction patterns of DPPC in the P_β phase for various water contents at higher angular resolution. An expanded view about the (1, 0) reflection is given. The percent water content is (*A*) 25, (*B*) 35, (*C*) 45, (*D*) 60, (*E*) 75. Temperature is 37.5°C in all cases.

phases for all water contents. Bragg spacings calculated from the (1,0) reflection differ from twice the Bragg spacing calculated from the (2,0) reflection by a maximum error of 0.84 Å (the 60% L_α measurement). The average error for the six measurements in the L_α and $L_{\beta'}$ phases is 0.33 Å. In the P_β phase, twice the Bragg spacing calculated from the (2,0) reflection falls between the spacing calculated for the two peaks in the (1,0) region. The (2,0) reflection is easily indexed as it is the most intense peak in the (2,0) region. Further, at 25% water content, the (2,0) spacing is consistent with the (3,0) spacing. The (3,0) reflection is the only reflection in the (3,0) region. For 45

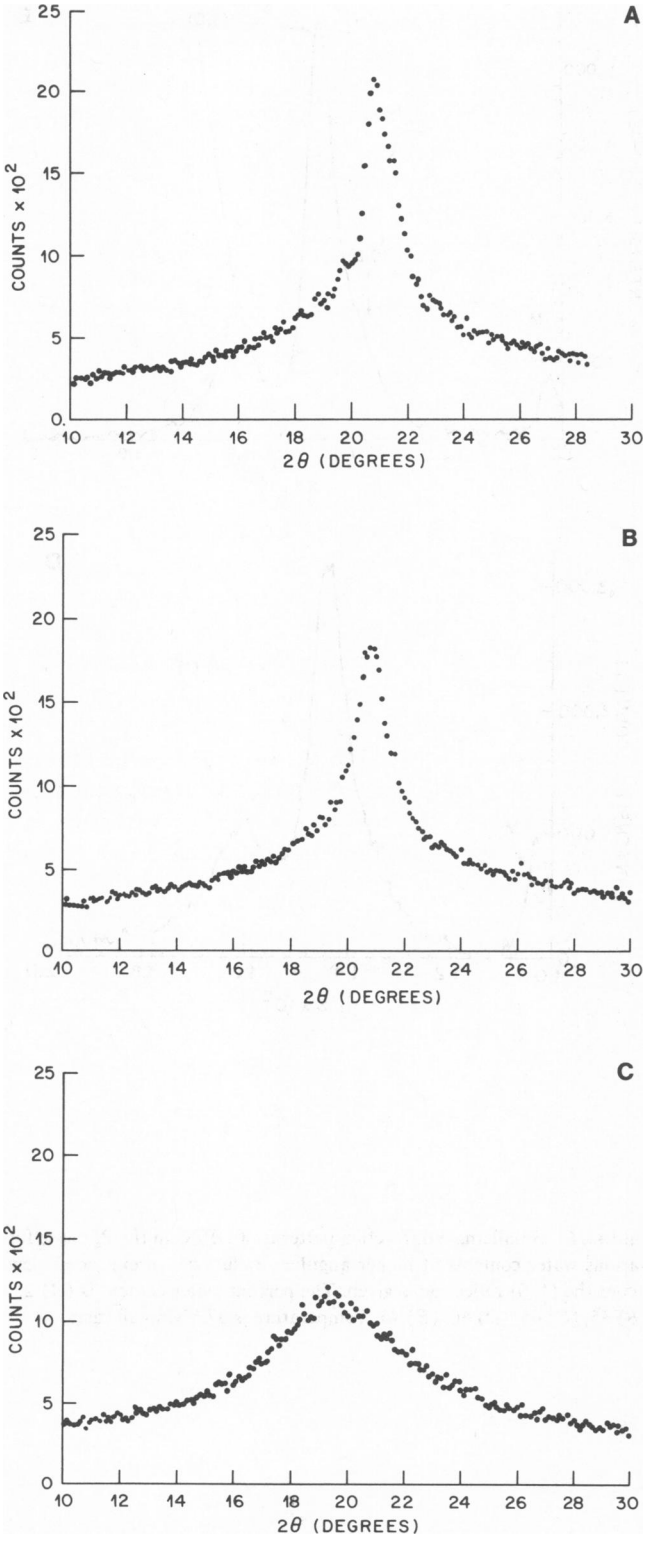

FIGURE 7 Large angle diffraction patterns of a 35% water content DPPC sample at various temperatures. (*a*) The sample is in the $L_{\beta'}$ phase at 27.3°C. The $(4.2\ \text{Å})^{-1}$ reflection is shown. Asymmetry of the peak indicates hydrocarbon chain tilting. (*b*) The sample is in the P_β at 37.5°C. The $(4.2\text{Å})^{-1}$ reflection has become symmetric indicating that the hydrocarbon chains have straightened. (*c*) The sample is in the L_α phase at 50.9°C. The broad diffraction band indicates that the hydrocarbon chains have melted.

TABLE I
X-RAY DIFFRACTION RESULTS
BRAGG SPACINGS USING THE POINT OF HALF INTEGRATED INTENSITY

Percent water content	Temperature	Phase	Diffraction order (1,0)	(2,0)	(2,0) × 2
	(°C)		(Å)	(Å)	(Å)
25	~23	$L_{\beta'}$	61.27	30.61	61.22
25	27.5	P_β	(59.81)* (61.00)*	30.61	61.22
35	23.5	$L_{\beta'}$	63.52	31.69	63.38
35	37.5	P_β	69.59 62.52	33.49	66.98
45	27.3	$L_{\beta'}$	63.97	31.76	63.52
45	37.5	P_β	70.82 62.28	33.73	67.46
45	46.0	L_α	65.09	32.36	64.73
60	27.3	$L_{\beta'}$	63.16	31.51	63.02
60	37.5	P_β	69.85 62.05	33.73	67.48
60	51.0	L_α	67.78	33.47	66.94

Spacings are calculated based on the peak's position relative to the attenuated incident beam. For resolved peaks, the point of half integrated intensity after removing a linear background is taken as the peak position.

*For the split peaks of the (1,0) reflection in the P_β phase at 25% water content, the position of the maxima of both peaks are given.

TABLE II
X-RAY DIFFRACTION RESULTS FOR THE P_β PHASE
BRAGG SPACINGS USING THE POINT OF PEAK INTENSITY

Percent water content	Temperature	Diffraction order (1,0)	(2,0)	(2,0) × 2
	(°C)	(Å)	(Å)	(Å)
25	37.5	59.81 61.00	30.53	61.06
35	37.5	62.38 69.06	33.31	66.62
45	37.5	62.28 70.32	33.56	67.11
60	37.5	62.42 69.35	33.50	67.00

and 60% water content samples, the (2,0) reflection is the only reflection in the (2,0) region. If the most intense peak of the (1,0) pair is compared with the (2,0) spacings, the average difference for the four determinations is +1.99 Å. If the least intense peak of the pair is compared with twice the (2,0) spacing, the average difference is −3.73 Å. These values fall well outside experimental error. (We have used the peak intensity for spacing determination, use of the point of half integrated intensity results in a difference of +2.01 and −4.12 Å for the two peaks.)

One possible explanation for these results is that the two peaks in the (1,0) region are the (1,0) and (1,1) reflections from the rippled bilayer lattice. It is notable that the (1,1) reflection would then be at least half an order of magnitude more intense than all the other (h, k) reflections with $k \neq 0$. It is also notable that the (1,1) reflection would then be the only reflection with $k \neq 0$ that is observed at higher water contents where disorder increases and signal decreases. However, if one insists on this indexing, the angle γ between the (0,1) and (1,0) reflection would need to be 90° to predict the observed spacings for the 35 and 45% examples. $\gamma = 90°$ would not account for the 25% measurements. To account for the 25% observations, the (0, 3) reflection (Fig. 2*a*) would also be indexed as the (1, 1) (i.e., overlapping peaks) and γ would become 97.8°. The two peaks in the (1, 0) region would then be (1,0) and (1, $\bar{1}$) reflections. This value of γ would not account for peaks observed at the high angle side of the (2,0) reflection. Indexing of these results is shown in Table III. Thus there does not appear to be an obvious method of indexing these powder patterns so that the two peaks are the (1,0) and (1,1) reflections.

Even if this were possible, the shifting of the (1,0) reflection is unexplainable. First, the shift is outside experimental error. Second, the shift cannot be due to the structure factor curve of flat bilayers of this lipid. Broad peaks that sample rapidly varying transforms can be shifted. However, many previous studies show that DPPC has a structure factor curve with an intense broad band that peaks at ~(45 Å).$^{-1}$ The (1,0) and (2,0) reflections sample this transform at either side of this main feature. Thus, the predicted shift would move the (1,0) reflection and (2,0) reflection together. We find that the two peaks move apart. Our results, both at lower angular resolution to (10 Å)$^{-1}$ and at higher angular resolution to (30 Å)$^{-1}$, show that reflections due to rippling become weaker and less well defined at higher water contents. However, splitting of the pair of peaks in the (1,0) region becomes more well defined at these higher hydrations. In summary, the possible explanation for these two peaks in the (1,0) region as simply the (1,0) and (1,1) reflections of the (h,k) lattice does not account for our observations.

The comparison of Bragg spacings and the observed increase in breadth of the peaks in this P_β phase suggests that the structure factor is zero near the (1,0) reflection. This zero, combined with the reflection width, results in a splitting and the formation of two peaks from one reflection. The fact that the intensity does not fall to the background level between those two peaks is due to finite angular resolution of this high resolution experiment and a finite range of ripple amplitudes as will be described.

The observed spacings are consistent with values

TABLE III
INDEXING OF THE 25% WATER CONTENT SAMPLE*

h	K	S^{-1} calculated	S^{-1} observed
		(Å)	(Å)
0	1	164‡	163.9
0	2	82	80.6
0	3	54.7	54.9
1	0	61.26	59.81 and 61.00
1	1	56.20	Not observed
1	$\bar{1}$	56.19	Not observed
2	0	30.63‡	30.63
2	$\bar{2}$	29.21	29.23
2	1	29.82	29.85
2	$\bar{3}$	27.35‡	27.35
3	0	20.42	20.41
3	K	—	Not observed

*Cell parameters: a = 61.26 Å, b = 164 Å, γ = 93.05°
‡Used to provide unit cell parameters

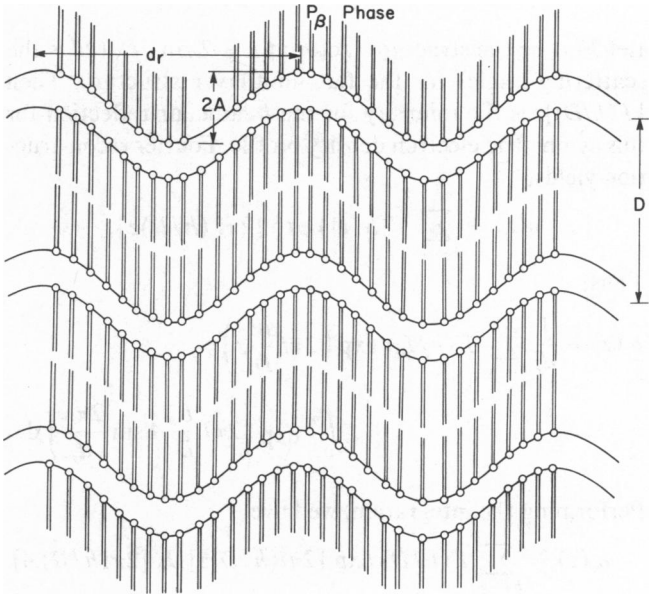

FIGURE 8 A schematic of the rippled P_β phase giving variables used in the calculation. d_r is the ripple wavelength and A is the amplitude. D is the multilayer repeat distance. The model is only a convenient form for calculation. Deviations from perfect sinusoidal behavior (such as the zigzag form suggested by Larsson [15]) should not produce major changes at small angles. The relation of this model to unit cell dimensions is as follows: $a = D$ and $b = d_r$. In this schematic $\gamma = 90°$. As an example $a = D$ = 61.26 Å, $b = d_r$ = 164 Å, and γ = 93.05° for the 25% water content sample at 37.5°C.
Detailed indexing for this case is given in Table III.

reported by Janiak et al. (4) at higher water contents. This spacing of 65.6 Å falls between the two peaks observed in this higher resolution experiment. At 25% water, our observed spacing of 60.78 Å compares favorably with neutron data (13).

Torbet and Wilkins (14) have carefully measured the structure of DPPC. They have taken care to account for changes in the structure upon swelling. This refined study clearly shows no zero in the structure factor curve at (~70 Å). However, rippling of the bilayer will alter the electron density profile projected on an axis orthogonal to the membrane. We proceed to calculate the effects of rippling.

Fig. 8 is a schematic of a rippled multilayer in which variables for the following calculation are depicted. Let $\rho(z)$ be the projected electron density of the flat multilayer of periodicity D. For simplicity, we describe the ripple as a simple sinusoidal wave of wavelength d_r and amplitude A. To compute the electron density of the rippled bilayer, $\rho_r(z)$, projected on the z-axis (the multilayering direction), we consider displacing a projection of the density for an infinitesimal in-plane area along the z-axis according to a sinusoidal modulation. This is equivalent to displacing the actual projected density for a flat bilayer along the z-axis according to this modulation. The electron density profile for the rippled phase is then

$$\rho_r(z) = \frac{1}{d_r}\int_0^{d_r} \rho\left[z + A\sin\left(\frac{2\pi x}{d_r}\right)\right] dx.$$

Let $F(s)$ be the structure factor at $s = 2\sin\theta/\lambda$ (2θ is the scattering angle) for the flat multilayer structure. Then $[F(h/D)]^2$ is the intensity for the h lamellar reflection for this symmetric electron density profile. Fourier reconstruction yields,

$$\rho(z) = \sum_{h=-\infty}^{+\infty} F(h/D)\exp[2\pi i\,(h/D)z].$$

Thus,

$$\rho_r(z) = \frac{1}{d_r}\sum_{h=-\infty}^{+\infty} F(h/D)\exp\left(2\pi i\frac{h}{D}z\right) \int_0^{d_r}\exp\left(2\pi i\frac{h}{D}A\sin\frac{2\pi x}{d_r}\right)dx.$$

Performing the integration, we have

$$\rho_r(z) = \sum_{h=-\infty}^{+\infty} F(h/D)\exp[2\pi i(h/D)z]\,J_0[2\pi(h/D)A].$$

In a method identical to developing the sampling theorem, we can calculate the structure factor for the rippled multilayer as follows

$$F_r(s) = 1/D\int_{-D/2}^{+D/2}\rho_r(z)\exp(-2\pi isz)\,dz.$$

Thus,

$$F_r(s) = \sum_{h=-\infty}^{+\infty} F\frac{h}{D}J_0\left[2\pi\frac{h}{D}A\right]\frac{\sin\pi D[(h/D)-s]}{\pi D[(h/D)-s]}.$$

At the ℓth lamellar reflection for the rippled structure, we have $F_r(\ell/D) = F(\ell/D)\,J_0[2\pi(\ell/D)A]$. Note that the above expression, which relates the rippled structure factor to the flat structure factor, does not depend in form on the details of the flat structure.

The flat bilayer structure is, in fact, a hypothetical structure. It contains all of the structural changes associated with P_β other than rippling. In comparison with $L_{\beta'}$, the structural changes that would produce major alterations at small angles are rippling and chain straightening. The flat bilayer structure is approximately related to the $L_{\beta'}$ bilayer structure by taking into account the tilt angle, α. As a rough estimate, we have $\rho(z) = \rho_{L_{\beta'}}(Z\cos\alpha)$.

Therefore,

$$F(s) = \frac{1}{D}\int_{-D/2}^{+D/2}\rho(z\cos\alpha)\exp(-2\pi isz)\,dz$$

$$= \frac{1}{D\cos\alpha}\int_{-D/2}^{+D/2}\rho(z)\exp\left[-2\pi\left(\frac{s}{\cos\alpha}\right)z\right]dz,$$

or

$$F(s) = \frac{F_{L_{\beta'}}(s/\cos\alpha)}{\cos\alpha}$$

so that

$$F_r(\ell/D) = \frac{F_{L_{\beta'}}\left(\frac{\ell}{D\cos\alpha}\right)}{\cos\alpha}J_0\left(2\pi\frac{\ell}{D}A\right).$$

For $\alpha \sim 30°$ in excess water (1) and $D \sim 67$ Å at 37.5°C in excess water, we have

$$\frac{1}{D\cos\alpha} = \frac{1}{67\text{ Å}(0.866)} = \frac{1}{58\text{ Å}}.$$

Thus, in this simple model, the rippled bilayer structure factor is related to the $L_{\beta'}$ structure factor by both a Bessel function term and by sampling at $(D\cos\alpha)^{-1}$.

Our data suggest that there is a zero very near $\ell/D \simeq 1/(67\text{ Å})$ for ≥ 35% water content. Previous work (12) shows that there is no zero at $\ell/D = 1/(67\text{ Å})$ for the $L_{\beta'}$ phase. Accounting for tilt moves the sampled point away from the nearest zero to $\ell/(D\cos\alpha) = 1/(58\text{ Å})$.

Experimental measurements (16) of the continuous structure factor curve for isolated UO_2^{++}-labeled bilayers at low concentrations might provide an experimental approximation for the flat bilayer structure. Recent studies (17) show that at concentrations of <1:10 UO_2^{++}/DPPC, tilt angle is removed. The structure factor curve at low UO_2^{++} concentration shows no zero at $\ell/D = 1/(67\text{ Å})$.

Thus, experimental or computational approaches suggest that the zero at 1/(67 Å) is not due to the flat bilayer's structure factor. We conclude that the zero must be due to the Bessel function factor.

The first zero in J_0 occurs at: $2\pi A/D = 2.4048$ or $A = 0.3827D$. For $D \simeq 67$ Å, $A = 25$ Å. If we take ~8 Å to be

TABLE IV
RIPPLE PARAMETERS

Percent water content	Temperature	d_r	A
	(°C)	(Å)	(Å)
25	37.5	164	23
35	37.5	145	25
45	37.5	147	25
60	37.5	—*	25

A, the ripple amplitude, is calculated from the equation $A = 0.3827D$ where D is taken as the minimum between the two peaks of the (1,0) reflection.
*(0,h) reflections were too weak to observe.

the lateral width of one lipid molecule, then for $d_r \simeq 160$ Å, there are 20 lipids in one wavelength. For an amplitude of 25 Å (50 Å peak-to-peak), this yields an average 2.5-Å displacement per hydrocarbon chain. This roughly equals the CH_2 repeat distance along the hydrocarbon chain.

The fact that this zero is maintained at 25% water where $D \simeq 61$ Å in the P_β phase, suggests that the amplitude, as well as the wavelength, changes with water content. Table IV gives the amplitude and wavelength of the observed ripples calculated by this method.

Quantitative agreement of the model with the data may be estimated as follows. Using the structure factor curve determined by Torbet and Wilkins (14), intensities at the $(D \cos \alpha)^{-1}$ sampling points may be multiplied by the appropriate Bessel function factors. For the 35% case, the zero (assigned from the minimum between the two peaks in the [1,0] region), is measured at $S = 0.01530$ Å^{-1}. This produces a value of 25 Å for the amplitude. The first peak of the (1,0) pair is found at $S = 0.01437$ Å^{-1}. At this point $J_0(2\pi SA)$ is found to be 0.0782. The (2,0) reflection is found at $S = 0.02985$ Å^{-1}, which corresponds to $J_0 \simeq -0.2708$. Using the Torbet and Wilkins (14) structure factor curve we estimate I_1/I_2 (at 67 Å cos 30° = 58 Å) to be between 56.25 and 11.11. Thus accounting for spherical disorientation by a Lorentz factor of 4, we find the calculated ratio, I_1/I_2, to fall between 17.81 and 3.52. (Note that the Bessel function factors must be squared.) The observed ratio, taken from peak heights, is 5.86. This falls within the range of values estimated from the structure factor curve. We also note that the ratio of squared Bessel functions at the two peaks in the (1,0) region is ~2, which compares roughly with the observed intensities. For the 25% case, I_1/I_2 is calculated to be 21.8 and we observe 20.4. This calculation is performed using a tilt of 20, which is based on the fact that maximum swelling ($D = 61$ Å) has not been reached.

Absolute intensities are not directly comparable. Onion-skinned multilayers, expected for the $L_{\beta'}$ phase, are undoubtedly disrupted to form flat multilayers with in-plane ripples at the pretransition. It can be shown that onion-skinned multilayers diffract x rays more weakly by a factor of the radius of the multilayer squared. Thus this expected morphological transformation prohibits comparing absolute intensities.

Our results are remarkably consistent with the theoretical predictions of Doniach (18) who extended Helfrisch's model (19) of spontaneous curvature. Rand et al.'s (6) observation of no tilt angle (confirmed by this study), really requires that η be > 1.0 in the Doniach theory. This automatically requires that the amplitude be a large fraction of the ripple period. Using Doniach's definition, the relative amplitude is $2A/d_r \sim 0.3$. For $\eta < 1$, the relative amplitude must be < 0.18. At $\eta \simeq 1 + \epsilon$, the relative amplitude is ~0.38. Therefore, our deduction of a relatively large ripple amplitude is consistent with no average tilt angle in the Doniach theory.

Our results also provide some insight concerning hydrocarbon chain tilt angle in the P_β phase. Although our model depicts the chains remaining parallel to the stacking direction (which is consistent with the wide angle diffraction results shown here and previously [6]), the large ripple amplitude produces as appreciable tilt angle with respect to the bilayer surface. Therefore the width of the bilayer need not dramatically increase to account for the observed increase in layer spacing. This is consistent with the study of Inoko and Mitsui (20). Our results do not support the electron density profile of this previous study (20). However, the profile was computed for DPPC in the presence of 5 mM $CaCl_2$, which may alter the ripple amplitude. Recent electron microscopy studies of negatively stained rippled bilayers also suggest that the amplitude of the ripple is very large (21).

McIntosh (22) has recently demonstrated that phospholipids with small head groups have no chain tilt. The suggested structural mechanism for tilted chains is the mismatch of areas in the bilayer plane between hydrocarbon chains and head groups. For DPPC, the larger head group requires a tilted hydrocarbon chain in order to eliminate voids in the structure. On the other hand, dipalmitoylphosphatidylethanolamine (DPPE) has a smaller head group and shows no chain tilt. In addition, DPPE does not have a pretransition.

Our measurement of amplitude suggests that rippling produces a large enough out-of-plane displacement to permit straight chains and a large head group. Rippling becomes the alternative structural solution to the area mismatch problem. Graddick et al.(7) have shown that about half the enthalpy of the pretransition is associated with a stacking disorder of the multilayer. The remaining enthalpy was attributed to an intrinsic intrabilayer process. Our results suggest that this process is rippling and is a direct consequence of area mismatch between hydrocarbon chains and head groups.

We gratefully acknowledge valuable discussions with S. Doniach, N. Gershfeld, W. Helfrich, J. F. Nagle, and P. Pershan. We particularly thank V. A. Parsegian for his suggestion of using excess water measure-

ments to rule out the possibility of another lipid phase. We also thank N. Albon for his help in lipid synthesis and for discussions on the nature of the pretransition. We appreciate the gift of DPPC from K. M. Keough for the lower angular resolution portion of this study. We thank P. Eisenberger for the use of his diffractometer for the wide angle studies. We gladly acknowledge the technical assistance of T. Bilash, S. Davey and W. C. Marra.

Received for publication 8 October 1980 and in revised form 9 November 1981.

REFERENCES

1. Tardieu, A., V. Luzzati, and F. C. Reman. 1973. Structure and polymorphism of the hydrocarbon chains of lipids: a study of lecithin-water phases. *J. Mol. Biol.*, 75:711–733.
2. Albon, A., and J. M. Sturtevant. 1978. Nature of the gel to liquid crystal transition of synthetic phosphatidylcholines. *Proc. Natl. Acad. Sci. U. S. A.* 75:2258–2260.
3. Powers, L., and P. S. Pershan. 1977. Monodomain, samples of dipalmitoyl phosphatidylcholine with varying concentrations of water and other ingredients. *Biophys. J.* 20:137–152.
4. Janiak, M. J., B. M. Small, and G. G. Shipley. 1976. Nature of the thermal pretransition of synthetic phospholipids: dimyristoyl and dipalmitoyllecithin. *Biochemistry.* 15:4575–4580.
5. Luna, E. J., and H. M. McConnel. 1977. The intermediate monoclinic phase of phosphatidylcholines. *Biochim. Biophys. Acta.* 466:381–392.
6. Rand, R. P., D. Chapman, and K. Larsson. 1975. Tilted hydrocarbon chains of dipalmitoyl lecithin become perpendicular to the bilayer before melting. *Biophys. J.* 15:1117–1124.
7. Graddick, W. F., J. B. Stamatoff, P. Eisenberger, D. W. Berreman, and N. Spielberg. 1979. Order-disorder and the pretransition of dipalmitoyl phosphatidylcholine multilayers. *Biochem. and Biophys. Res. Commun.* 88:907–712.
8. Selinger, Z., and Y. Lapidot. 1966. Synthesis of fatty acid anhydrides by reactions with dicyclohexylcarbodiimide. *J. Lipid Res.* 7:174–175.
9. Singleton, W. S., M. S. Gray, M. L. Brown, and J. L. White. 1965. Chromatographically homogeneous lecithin from egg phospholipids. *J. Am. Oil Chem. Soc.* 42:53–56.
10. Chadha, J. S. 1970. Preparation of crystalline L-α-glycerophosphorylcholine-cadmium chloride adduct from commercial egg lecithin. *Chem. Phys. Lipids.* 4:104–108.
11. Cubero, R. E., and D. vanden Berg. 1969. Synthesis of lecithins by acylation of o-(*Sn*-glycero-3-phosphoryl) choline with fatty acid anhydride. *Biochim. Biophys. Acta.* 187:520–526.
12. Janiak, M. J., D. M. Small, and G. G. Shipley. 1979. Temperature and compositional dependence of the structure of hydrated dimyristoyl lecithin. *J. Biol. Chem.* 254:6068–6078.
13. Buldt, G., H. U. Gally, A. Sealig, and J. Sealig. 1978. Neutron diffraction studies on selectively deuterated phospholipid bilayers. *Nature (Lond.).* 271:182–184.
14. Torbet, J., and M. H. F. Wilkins. 1976. X-ray diffraction studies of lecithin bilayers. *J. Theor. Biol.* 69:447–458.
15. Larsson, K. 1977. Folded bilayers—an alternative to the rippled lamellar lecithin structure. *Chem. Phys. Lipids.* 20:225–228.
16. Stamatoff, J., T. Bilash, Y. Ching, and P. Eisenberger. 1979. X-ray scattering from labeled membranes. *Biophys. J.* 28:413–421.
17. Parsegian, V. A., R. P. Rand, and J. Stamatoff. 1981. Perturbation of membrane structure by uranyl acetate labeling. *Biophys. J.* 33:475–477.
18. Doniach, S. 1979. A thermodynamic model of the monoclinic (ripple) phase of hydrated phospholipid bilayers. *J. Chem. Phys.* 70:4587–4596.
19. Helfrich, W. 1974. The size of bilayer vesicles generated by sonication. *Phys. Lett. A.* 50:115–116.
20. Inoko, Y., and T. Mitsui. 1978. Structural parameters of dipalmitoyl phosphatidylcholine lamellar phases and bilayer phase transitions. *J. Phys. Soc. Jap.* 44:1918–1924.
21. McIntosh, T. J., and M. J. Costello. 1981. Effects of n-alkanes on the morphology of lipid bilayers: freeze fracture and negative stain analysis. *Biochim. Biophys. Acta.* 645:318–326.
22. McIntosh, T. J. 1980. Differences in hydrocarbon chain tilt between hydrated phosphatidylethanolamine and phosphatidylcholine bilayers. *Biophys. J.* 29:237–246.